Revista Brasileira de Física, Vol. 18, nº 4, 1988

# Virtual Photon Spectra for Finite Nuclei

E. WOLYNEC and M.N. MARTINS
*Instituto de Física, Universidade de São Paulo, Caixa Postal 20516, São Paulo. 01498, SP, Brasil*

**Recebido em 5 de Julho de 1988**

Abstract The experimental results of an isochromat of the virtual photon spectrum, obtained by measuring the number of ground-state protons emitted by the 16.28 MeV isobaric analogue state in $^{90}Zr$ as a function of electron incident energy in the range 17-105 MeV, are compared with the values predicted by a calculation of the E1 DWBA virtual photon spectra for finite nuclei. It is found that the calculations are in excellent agreement with the experimental results. The DWBA virtual photon spectra for finite nuclei for E2 and M1 multipoles are also assessed.

## 1. IMTRODUCTION

The interest in electrodisintegration experiments to study the multipolarity of nuclear transitions has motivated an experiment to test virtual photon calculations with great accuracy. An isochromat of the E1 virtual photon spectrum was measured by couting the number of ground state protons, emitted by the 16.28 MeV, 1-, isobaric analogue state in $^{90}Zr$. as a function of incident electron energy in the range 17-105 MeV[1]. When this experiment was performed. available virtual photon spectra were evaluated taking into account the distortion of incoming and outgoing electron waves in the Coulomb field of a point nucleus. It had already been shown that the plane wave approximation could only be used for very light nuclei and that the distorted wave Born approximation (DWBA) calculations[2] yielded spectra of correct magnitude as a function of Z. However. there were doubts about the range of validity of the point nucleus approximation. Since in electrodisintegration experiments the outgoing electrons are not detected. the measurements integrate over all possible values of momentum transfer. Because the electron scattering cross section is forward peaked. the electrodisintegration cross section is dominated by low momentum transfer and it was often argued that size corrections should be negligible. The isochromat experiment showed that for an E1 transition in a medium weight nucleus such as $^{90}Zr$. size effects become evident for electrons of incident energy greater than 30 MeV. At that time two types of size corrections were available. One based on a plane wave calculation[1,3] and also an evaluation of virtual photon spectra for a finite nucleus, using a model for nuclear charge and current distributions, but performed in second order Born approximation (SOBA)'. It was found[1,5] that both size corrections yielded acceptable results, but SOBA made a prediction closer to the experimental values. However SOBA is inadequate to describe heavy nuclei because these require a DWBA calculation. More recently Zamani-Noor and Onley[6] have developed DWBA virtual photon calculations for finite nuclei. The comparison of their results with experimental data for the (e,n) cross section in $^{181}Ta$ is discussed in ref.5. However the isochromat data of ref.1 is a more precise test for the virtual photon calculation. The purpose of this paper is to compare the experimental results of ref.1 with the E1 DWBA calculations for finite nuclei[6]. The results of these calculations for other multipoles will also be discussed.

## 2. THE VIRTUAL PHOTON METHOD

The virtual photon method relates electro- and photodisintegration through virtual photon spectra. In photodisintegration experiments, the photon is simply a means of injecting a certain amount of energy and angular momentum into the nucleus, which then has a variety of channels through which it may decay. het us assume we are dealing with an Uranium nucleus and that it chooses the fission channel. We may draw diagramatically the process of photofission as in fig. 1(a). The same nucleus can interact with a passing electron, which will create a time-varying field at the target site and this field rnay be regarded as a pulse of electromagnetic radiation. This is an old idea in classical electrodynarnics due to Weiszacker[7] and Williams[8], but in quantum mechanics the intermediate radiation is a virtual photon and the process is depicted as in fig. 1(b). The nuclear part of the diagram is the same as in fig. 1(a). In both cases the interaction is electromagnetic, but there are important differences that force the nucleus to reveal more about itself, when interacting with an electron, than in a real photon interaction. Notice that the electron lines are curved because the electrons are moving in a Coulomb field which for a heavy nucleus can distort the electron wave function considerably.

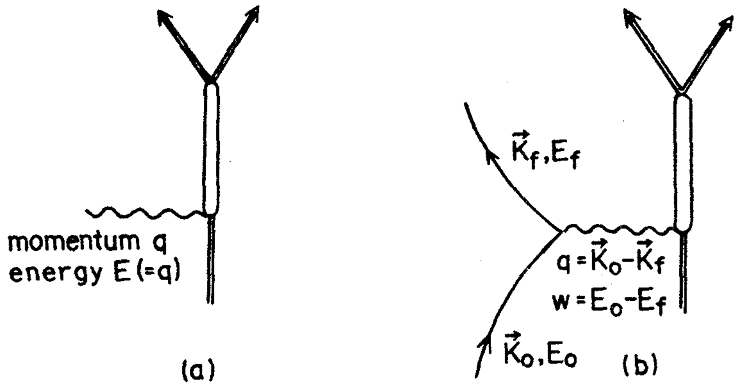


**Fig.1** - The photofission process (a) and the electrofission process (b) are shown diagramatically.

The experimentalist has the choice of using real or virtual photons. Both originate with electrons, but real photons are created separately in a converter foil (see fig. 2) and travel a long path to the target. In this case the target experiences radiation with a broad spectrum which is known as the bremsstrahlung spectrum. On the other hand. a virtual photon is created and absorbed in interaction with one and the same nucleus, which is thus both converter and target. In a sense the target is, in this case, just closer to the source. If we make a classical analogy and think of the electron as an antenna. which is emitting electromagnetic radiation, there is the familiar difference between near field and far field. Far field radiation is purely transverse and has effectively a plane wave front: near field radiation is not planar, and has also longitudinally polarized components. Near field or virtual radiation also has a different spectrum from bremsstrahlung and the shape and magnitude of this spectrum has to be known in order to analyze electrodisintegration measurements. Onley and his c collaborators[4,6,9,10] have generated the virtual photon spectra in the distorted wave approximation, first using a numerical calculation that treats the nucleus as a point[9,10] and more recently for finite nuclei[4,6].

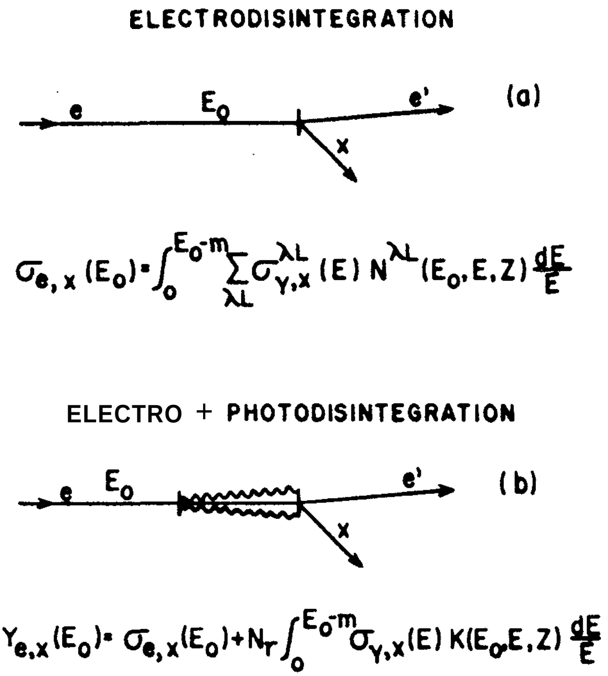


Fig.2 - Schematic view of an electrodisintegration experiment (a) and photodisintegration experiment (b).

If the nucleus is subjected to a beam of radiation with spectrum $N(E)$ the resulting cross section is

$$\sigma = \int N(E)\sigma_\gamma(E)\frac{dE}{E} \tag{1}$$

where $\sigma_\gamma(E)$ is the photoexcitation cross section as a function of photon energy E $(h = c = 1)$ and $N(E)/E$ is the number of incident photons per unit energy interval. In the case of bremsstrahlung photons the spectrum depends on the electron incident energy $E_0$, the atomic number $Z$ of the converter or radiator and the number $N_r$ of atomic nuclei/cm$^2$ in the radiator. In this case eq.(1) becomes

$$\sigma(E_0) = N_r \int_0^{E_0-m} \sigma_\gamma(E)K(E_0,E,Z)\frac{dE}{E} \tag{2}$$

where m is the electron rest energy. $K(E_0, E, Z)$ is the bremsstrahlung cross section and thus $N_r K(E_0, E, Z)/E$ is the number of photons per unit energy interval.

In the virtual photon case. assuming that the scattered electron is not detected (inclusive experiments like electrodisintegration) the cross section is rather similar to eq.(2).

$$\sigma(E_0) = \int_0^{E_0 - m} \sum_{\lambda L} N^{\lambda L}(E_0, E, Z) \sigma_\gamma^{\lambda L}(E) \frac{dE}{E} \tag{3}$$

Here $\lambda L$ stands for the spin and parity or multipole class of the electromagnetic transition.

The basic difference is ehat the plane wave real photon spectrum has the same strength in all multipoles and in eq.(2):

$$\sigma_\gamma(E) = \sum_{\lambda L} \sigma_\gamma^{\lambda L}(E) \tag{4}$$

The virtual photon spectra by contrast, increase rapidly with L as illustrated in fig.3, which shows $N^{EL}$ for EL $= E1, E2,$ and E3 for $E_0 = 30$ MeV in tantalum. This enhancement has already been exploited in various experiments to examine multipole transitions of orders higher than $E1$. which a real photon spectrum does not reveal (e.g. references (11-22)). Combining electro- and photodisintegration measurements the experimentalist can change the multipole composition seen by the target.

b) Calculation of virtual photon spectra

In order to discuss the accuracy of the calculations we review them briefly.

For any system which interacts with the electromagnetic field the interaction may be written in the form

$$H_{int} = \int (\vec{J} \times \vec{A} - \rho\phi) d^3r \tag{5}$$

where Ã, and 4 are the potentials created by the electron. The nucleus is represented by the nuclear current density $\vec{J}$ and transition charge densíty p. These are constrained by continuity

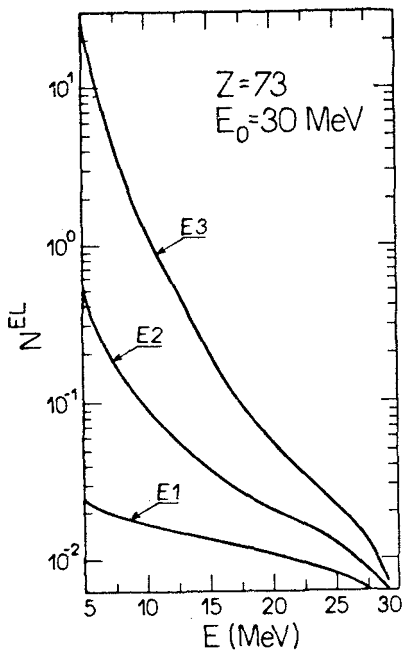


Fig.3 - E1, E2 and E3 DWBA virtual photon spectra for a finite nucleus.

$$\vec{\nabla} \times \vec{J} + (d\rho/dt) = 0 \tag{6}$$

Since electrons are scattered by the Coulomb field of the nucleus the distorted wave (DWBA) formalism is used. Thus the static part of the Coulomb field is included in the unperturbed hamiltonian and hence $H_{int}$ includes only the radiative part of the interaction.

Electron wave functions obey the Dirac equation and the DWBA formalism breaks the wave functions into partial waves. These are labelled with the Dirac angular momenturn quantum nurnber $K$, which rnay be a positive or negative integer and specifies both the total (j) and the orbital (L) quantum numbers

$$j = |K| - 1/2 \qquad and \qquad \ell = |K + 1/2| - 1/2 \tag{7}$$

The basic probability amplitudes for the electron to change from angular momentum state $K_0$, to state $K_f$, while emitting a photon in state $\lambda L$ are called

$R^{\lambda L}(K_0,K_f)$. In terms of these. the virtual photon spectra of eq.(3) can be obtained[4,6,9,10]

$$N^{\lambda L}(E_0,E,Z)=\frac{\alpha}{\pi}\frac{K_f}{K_0}\frac{(E_0+m)(E_f+m)E^4}{2L+l}$$
$$\times\sum_{K_0K_f}(2j_0+1)(2j_f+2)|(j_0,j_fL;-1/2,1/2)R^{\lambda L}(K_0,K_f)|^2 \tag{8}$$

Here $E_f$ is the electron final energy and a is the fine structure constant.

In the point nucleus approximation the electron does not penetrate the nucleus and in the plane wave approximation the distortion of electron waves is ignored. Under both approximations the calculation of $N^{XL}$ is relatively simple and one obtains analytical expressions for them[4]. However. the approximations will work for suitably low $Z$ nuclei so that the distortion in electron waves is negligible. It can be used when the Coulomb energy is small compared with the incident electron energy:

$$\frac{\alpha Z}{R_N}<<E_0 \tag{9}$$

In eq.(9) $R_N$ is the nuclear radius. The assumption that the nuclear and electron waves do not interpenetrate significantly amounts to a condition

$$\bar{q}R_N<<1$$

where $\bar{q}$ is the average momentum transfer. How stringent this is depends on the process we are looking at. being least for magnetic and electric dipoles, for which the electron angular distribution exhibits a strong forward peak and for light nuclei (small $R_N$).

For medium and heavy nuclei conditions eqs. (9) and (10) are inevitably violated, and to evaluate $R^{XL}$ in DWBA for a finite nucleus we have to assume a model to describe nuclear density functions for values of $r<R_N$, because $R^{\lambda L}$ involves an integral over all space (electron coordinates).

It has been shown[4] that the results are not particularly sensitive to the details of the charge distribution. This should be expected since electron scattering at low momentum transfer $(E_0 \lesssim 150 MeV)$ is unable to detect the details of the charge distribution and the only quantity that can be extracted from such experiments in the nuclear root-mean-square radius. In order to evaluate virtual photon spectra for finite nuclei. Onley and collaborators[4] take the ground state charge distribution $\rho(r)$ to be the standard Fermi shape.

The transition probabilities $R^{\lambda L}$ contain the radial parts of the nuclear matrix elements, $R_N^{EL}$ and $R_N^{ML}$, in which the nuclear current densities are expanded in multipoles (for details see ref.6). Thus

$$R_N^{EL} = \int_0^{R_N} \{ - j_{L+1}(E_0 r')|L/(L+1)|^{1} \\ j_{L+1}(r') + j_{L-1}(E_0 r') J_{L-1}(r') \} r'^2 dr' \tag{11}$$

and

$$R_N^{ML} = \int_0^{R_N} j_L(E_0 r') J_L(r') r'^2 dr' \tag{12}$$

where $j_L$ is the spherical Bessel function.

For the nuclear current densities Zamani-Noor and Onley use:

$$J_{L-1}(r) = r^{L-1} \rho_0(r) \tag{13}$$

$$J_L = d\rho_0/dr \tag{14}$$

and

$$J_{L+1} = 0 \tag{15}$$

which are derived under the assumption of irrotational incompressible flow in the nucleus.

The great difficulty in evaluating virtual photon spectra in DWBA is that the evaluation of $R^{XL}$ requires to perform an integral over all space. Since the interaction involved is electromagnetic. and therefore long-ranged. there is no mechanism for cutting off this integral. To overcome this, Onley and his collaborators[6,10] have developed an assymptotic series for the remote part of the integral and use numerical integration for the near part.

## 3. TESTS OF DWBA VIRTIJAL PHOTON SPECTRA FOR FINITE NUCLEI

### a) The E1 spectrum

In ref.1 the cross section $\sigma_{e,p_0}(E_0)$ for the proton decay of the 16.28 MeV, 1-, isobaric analogue state in $^{90}Zr$ was measured as a function of incident electron energy in the range 17-105 MeV. The same decay was also measured using bremsstrahlung photons.

The photonuclear absorption cross section integrated over the level width of the 16.28. 1-, isobaric analogue state in $^{90}Zr$ that results in protons populating the ground state of $^{89}Y$ is related to the photon width. $\Gamma_\gamma$, the ground state proton width, $\Gamma_{p_0}$, and the total width, $\Gamma$, of this level by

$$\int \sigma_{\gamma,p_0}(E)dE = (\pi\bar{\lambda})^2[(2I+1)/(2I_0+1)]\Gamma_{p_0}\Gamma_\gamma/\Gamma \tag{16}$$

where $I$ and $I_0$ are the spins of the excited and ground states.

Since

$$\sigma_{e,p_0}(E_0) = (1/E)[N^{E1}(E_0,E,Z)] \int \sigma^{E1}_{\gamma,p_0}(E)dE \tag{17}$$

using eqs.(16) and (17) with the experimental results for a $(E_0)$ and calculating $N^{E1}(E_0, 16.28, 40)$, the invariant quantity $\Gamma_{p_0}\Gamma\gamma/\Gamma$ can be obtained. By an analogous procedure. replacing in eq.(17) the number of virtual photons per unit energy interval by the appropriate number of real photons, the same invariant quantity $\Gamma_{p_0}\Gamma_\gamma/\Gamma$ can be obtained from the photoexcitation measurements. In ref.1 it was found that using DWBA E1 virtual photon spectra for a point nucleus. the value of this invariant quantity decreased as the electron energy increased, departing from that determined from the photoexcitation measurement, showing clearly that size corrections were necessary. When the virtual photon spectra were evaluated in the second order Born approximation. taking into account the finite size of the nucleus[4]. then the results obtained for $\Gamma_{p_0}\Gamma_\gamma/\Gamma$ were constant with the electron incident energy and compatible with that obtained from photodisintegration. The results obtained are

$$65.4 \pm 0.6 \ eV \quad \textit{from photodisintegratton}$$
$$66.1 \pm 0.3 \ eV \quad \textit{from electrodisintegration using SOBA}$$

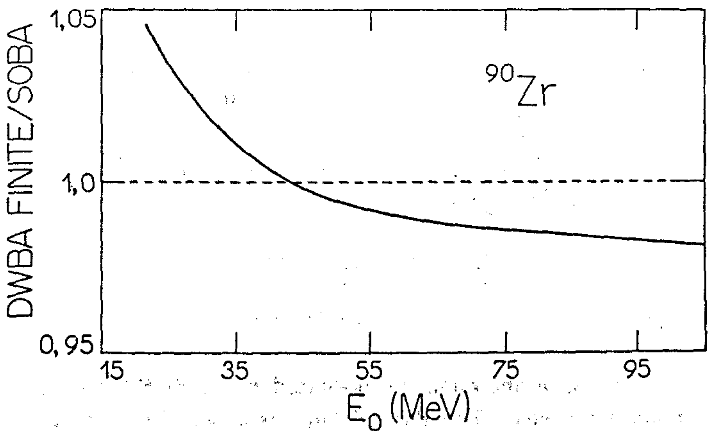


Fig.4 - Ratio between the number of 16.28 MeV E1 virtual photons obtained with DWBA for a finite nucleus and that obtained with SOBA.

In fig.4 we show the ratio between the number of 16.28 MeV E1 photons obtained using DWBA for a finite nucleus[6] and that obtained using SOBA. For $E_0 = 17.5$ MeV the number of virtual photons predicted by DWBA for a finite nucleus is 4 percent bigger than that predicted by SOBA. This can be understood because distortion is more important for lower values of the electron incident energy and indicates that the second order Born approximation does not take completely into account the distortion effects in $^{90}Zr$. At 105 MeV SOBA underestimates size corrections by 2 percent.

Fig. 5 shows $\Gamma_{p_0}\Gamma_\gamma/\Gamma$ evaluated using SOBA and DWBA for a finite nucleus. In both cases $\Gamma_{p_0}\Gamma_\gamma/\Gamma$ is constant and independent of the electron incident energy. The dashed lines represent in each case the weighted average vaiue, which are:

65.2 ± 0 . with **DWBA for** a finite nucleus and 66.1 ± 0.3 **eV** for **SOBA.** Compared to **65.4** ± 0.6 **eV** obtained from photodisintegration, the DWBA **result** is in better agreement.

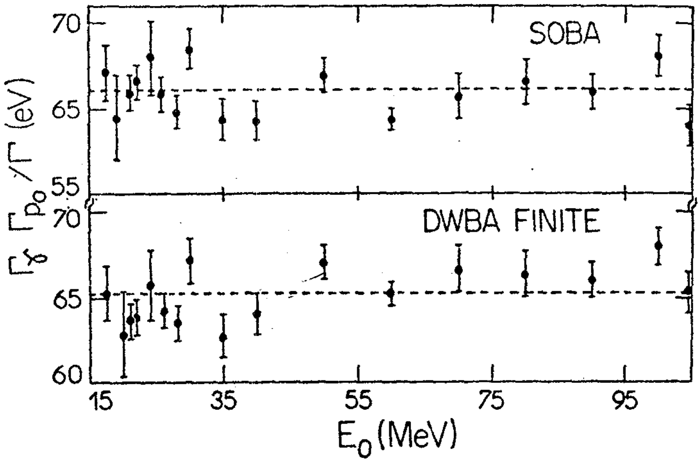


**Fig.5** - The **invariant** quantity evaluated using **SOBA** and DWBA **for** a finite nucleus. The dashed **lines** represent in each case the weighted average value.

We conclude that the E1 virtual photon spectra evaluated in DWBA for a finite nucleus is in excellent agreement with experiment.

b) The **E2** spectrum

There is no known **E2** isslated **level** in **medium** weight or heavy **nuclei** which decays by particle emission. Thus an isochromat of the **E2** spectrum cannot **be** measured.

**In** ref. 5 the electrodisintegration of $^{181}$**Ta** by one neutron emission was used to assess the reliability of the recent **DWBA** calculations for a finite nucleus. In $^{181}$**Ta** the isoscalar **E2** resonance decays dominantly by one neutron emission **be**cause charged particle decay is inhibited by the Coulomb barríer. Thus the (e, n) cross section contains **basically E1** and **E2** excitations. Figs. **6** and 7 show E1 and **E2** DWBA virtual photon spectra for a point and finite nucleus ($Z$ = 73).

Size corrections affect the E2 spectrurn far more. It was shown[6] that the use of virtual photon spectra for a point nucleus rnade electro- and photodisintegration incornpatible in heavy nuclei, but those for a finite nucleus yielded good agreernent with experiment. The DWBA calculations for a finite nucleus[6] make electrodisintegration and photodisintegration cornpatible and the E2 strength necessary to sirnultaneously fit both cross sections is in good agreement with the known systematics.

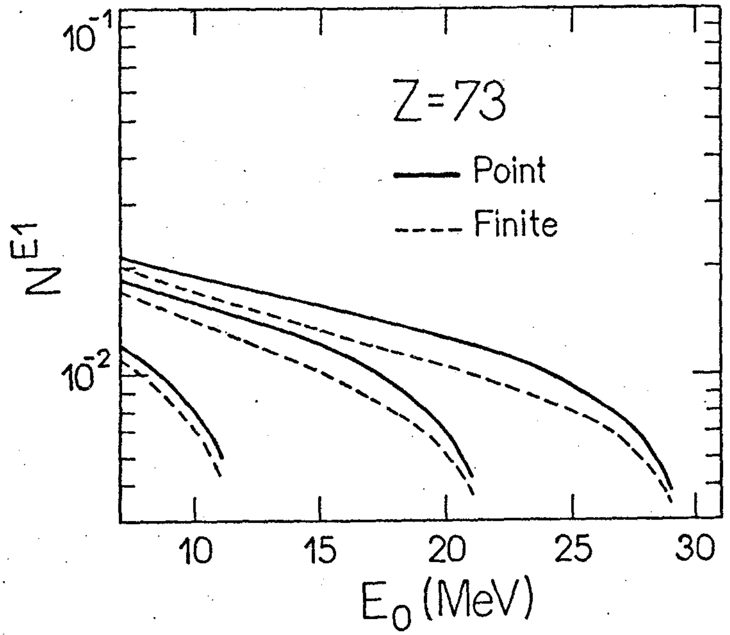


**Fig.6 - DWBA E1** virtual photon spectra for a point and a finite nucleus.

This test does not have the same accuracy as the rneasurement of the **E1** isochromat. but it indicates that the **E2** size correction has the appropriate rnagnitude.

The **M1** Spectrum

Fig. 8 shows **DWBA M1** spectra for a point and a finite nucleus ($Z = 73$). The magnitude of the size correction is rnuch bigger for **M1** than for **E2** (see fig.

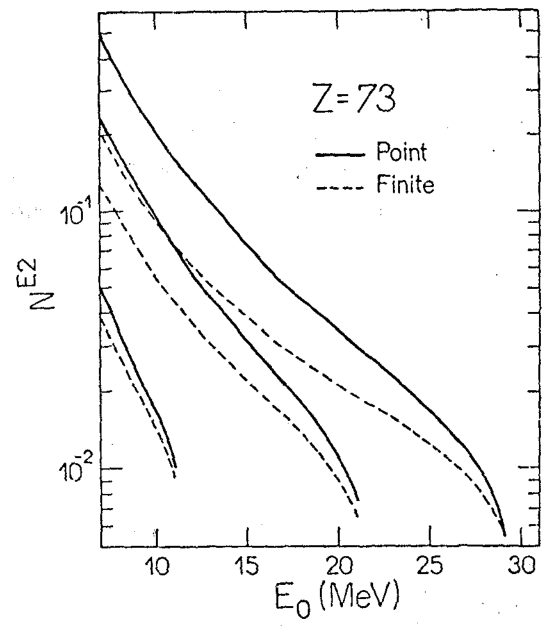


Fig.7 - DWBA E2 virtual photon spectra for a point and a finite nucleus.

7). This is surprising if one reasons along lines suggested by plane wave (PWBA) calculations. In PWBA size effects are small for the transverse components of the virtual photon spectra[3] and this behaviour is reproduced by DWBA. at least for E1 and E2 spectra. The PWBA E1 spectrum is dominantly transverse and the magnitude of its size corrections in DWBA is relatively small as compared to that of the E2 spectrum, which is domínantfy longitudinal[3,5]. Since the PWBA M1 spectrum is purely transverse, size corrections should have little effect on the corresponding DWBA virtual photon spectrum.

In a recent paper on $^{197}$Au. Campos *el al.*[24] derived the M1 and E2 strengths observed on the one neutron decay channel of the photonuclear cross sections. They used both finite and psint DWBA M1 spectra in their analysis and got consiotent results only with the point DWBA M1 spectrum. It must be emphasized that both E1 and E2 spectra used in the analysis were finite DWBA calcuiations. The Ml cross section obtained using finite DWBA M1 spectra was too big (larger

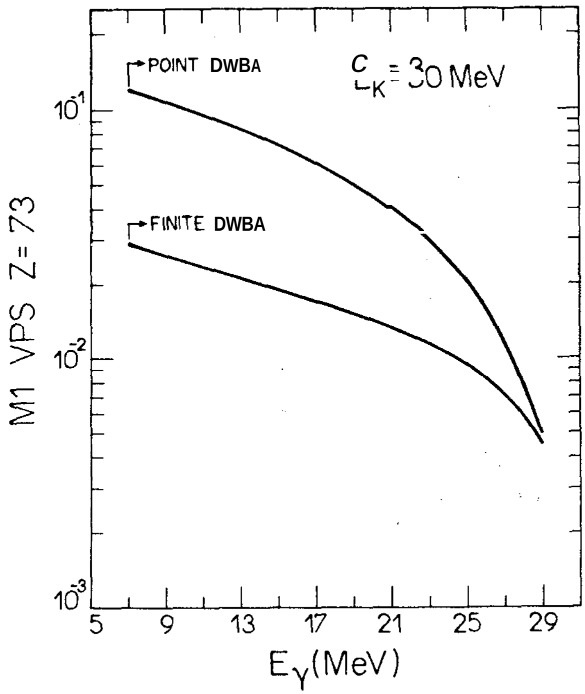


Fig.8 - DWBA M1 virtual photon spectra for a point and a finite nucleus.

than the absorption in the energy region studied). probably due to the excessive correction on the spectrum, which made it too small. The results obtained for M1 strength using point DWBA M1 spectra were compatible with previous experimental results and with theoretical estimates and suggest that the spectra used in the analysis have the correct magnitude.

## 4. CONCLUSIONS

The E1 virtual photon spectra evaluated in the distorted wave Born approximation for a finite nucleus are in excellent agreement with experimental results.

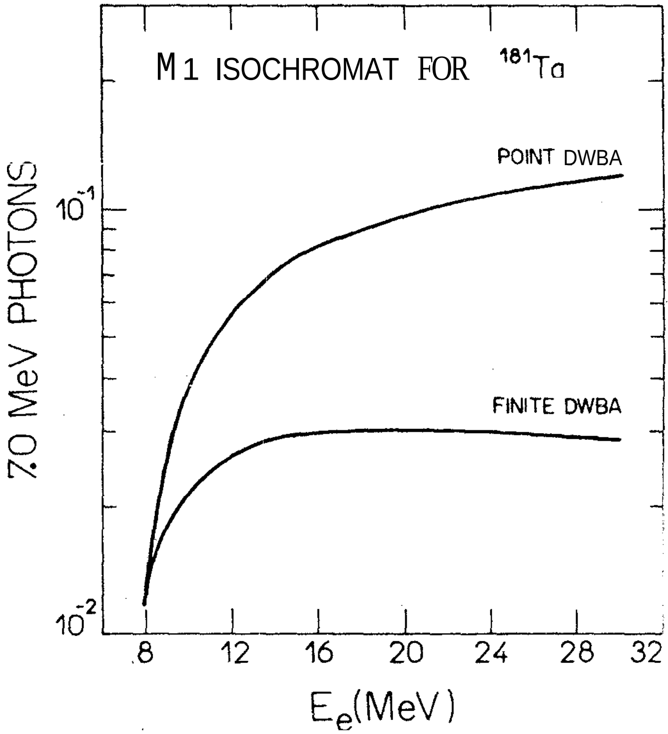


Fig.9 - Isochromats of the DWBA M1 virtual photon spectra for a point and a finite nucleus. The virtual photon energy is 7 MeV and the target nucleus is Z=73.

The E2 spectra are also in good agreement with experimental results, but the experimental test in this case does not have the same accuracy as that for the El.

For magnetic multipoles the results of the calculations for a finite nucleus seem to be unreliable. They predict a very large correction due to the finite size of the nucleus, while these corrections are expected to be very small as a consequence of the transverse nature of these multipoles. The failure of the calculations for a finite nucleus may result from inadequate model description of the nucler currents. Eventhough this strongly affects the magnetic multipoles, it has little effect on the electric multipoles. For the latter it is found[4,6] that the results are rather independent of the detailed shape of the charge distribution.

They depend primarily on the values of the nuclear root-mean-square radius and the appropriate transition radius.

For magnetic multipoles the most reliable calculation available present at is the DWBA for a point nucleus. For the M1 multipole it yields B(M1) strengths. derived from electrodisintegration measurements. which are consistent with results obtained with other probes. like polarized photon scattering.

REFERENCES


1. W.R. Dodge. E. Hayward and E. Wolynec. Phys. Rev. C28. 150(1983).
2. I.C. Nascimento. E. Wolynec and D.S. Onley. Nucl. Phys. A246. 210 (1975).
3. A.C. Shotter. J. Phys. G: Nucl. Phys. 5, 371 (1979).
4. P. Durgapal and D.S. Onlèy. Phys. Rev. C27. 523 (1987).
5. E. Wolynec. V.A. Serr/ ao and M.N. Martins. J. Phys. G: Nucl. Phys. 13, 515 (1987).
6. F. Zamani-Noor and D.S. Onley. Phys. Rev. C33. 1354 (1986).
7. K.F. Weiszacker. Z. Physik 88. 612 (1934).
8. E.J. Williams. Phys. Rev. 45. 729 (1934).
9. W.W. Gargaro and D.S. Onley. Phys. Rev. C4. 1032 (1971).
10. C.W. Soto Vargas. D.S. Onley and L.E. Wright, Nucl. Phys. A288. 45 (1977).
11. E. Wolynec, W.R. Dodge. R.G. Leicht and E. Hayward. Phys. Rev. C22. 1012 (1980).
12. W.R. Dodge. R.G. Leicht. E. Hayward and E. Wolynec, Phys. Rev. C24. 1952 (1981).
13. D.M. Skopik. J. Asai and J.J. Murphy II. Phys. Rev. C21. 1746 (1980).
14. T. Tamae. T. Urano. M. Hiroka and M. Sugawara. Phys. Rev. C21. 1758 (1980).
15. A.G. Flowers. D. Brandford. J.C. McGeorge. A.C. Shotter, P. Thorley and C.H. Zimmerman. Phys. Rev. Lett. 43. 323 (1979).
16. J.D.T. Arruda Neto, S.B. Herdade, I.C. Nascimento and B.L. Berman, Nucl. Phys. A389. 378 (1982).
17. J. Aschenbach, R. Haeg and H. Krieger. Z. Phys. A292. 285 (1979).

18. H. Stroher. R.D. Fisher, J. Drexler, K. Huber, U. Kneissl. R. Batzek. H. Ries, W. Wilck and H.J. Maier, Phys. Rev. Lett. **47**, 318 (1981).
19. H. Stroher. R.D. Fisher. J. Drexler, K. Huber, U. Kneissl. R. Batzek, H. Ries. W. Wilck. and H.J. Maier. Nucl. Phys. **A378**, 237 (1982).
20. E. Wolynec. W.R. Dodge and E. Hayward. Phys. Rev. Lett. **42**, 27 (1979).
21. M.N. Martins. E. Wolynec and M.C.A. Campos. Phys. Rev. **C26**, 1941 (1982).
22. W.R. Dodge, E. Hayward. M.N. Martins and E. Wolynec. Phys. Rev. **C32**, 781 (1985).
23. M.I.C. Cataldi, M.Sc. Thesis, Instituto de Flsica, Universidade de São Paulo (1986).
25. M.C.A. Campos. M.Sc. Thesis, Instituto de Física, Universidade de São Paulo (1986) and M.C.A. Campos, E. Wolynec and M.N. Martins. J. Phys. G: Nucl. Phys. **14**, 1139 (1988).

**Resumo**

Os resultados experimentais referentes à medida de uma isocromata do espectro de fótons virtuais. a qual foi efetuada detectando-se o número de prótons que decaem para o estado fundamental, emitidos pelo estado análogo de energia 16.28 MeV no $^{90}Zr$. em função da energia do elétron incidente na faixa de 17-105 MeV, são comparados com os valores previstos pelo cálculo do espectro de fótons virtuais E1, efetuado na aproximação DWBA e considerando o tamanho finito do núcleo. Verifica-se que os cálculos estão em excelente acordo com os resultados experimentais. Os cálculos de espectros de fótons virtuais. em DWBA e para núcleos finitos. para multipolos E2 e M1 tambdm são discutidos.